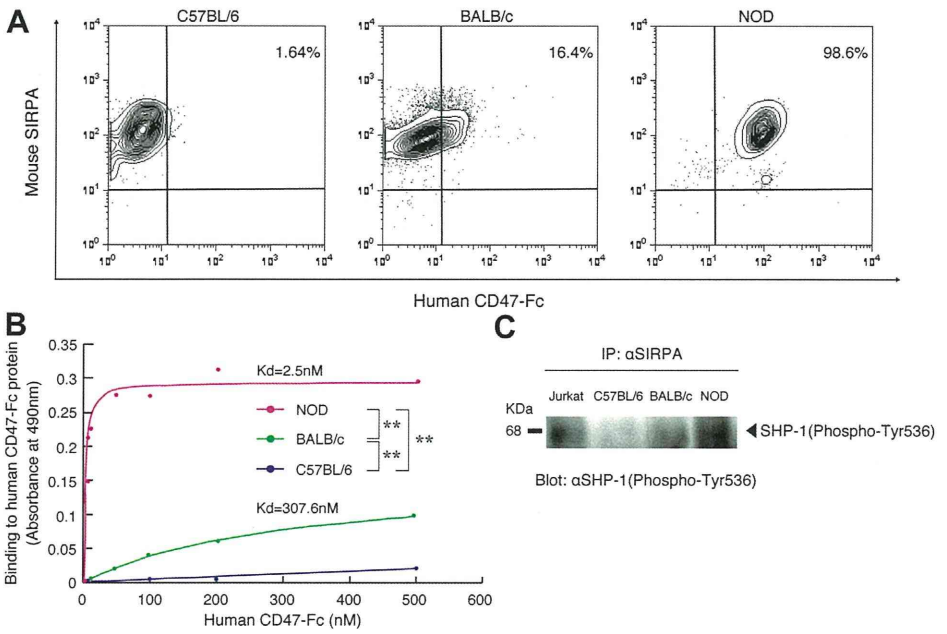

Figure 1. Binding capability of mouse SIRPA to human CD47. **(A)** Binding of the human CD47-Fc fusion protein to SIRPA-expressing macrophages derived from C57BL/6, NOD, and BALB/c mice by flow cytometry analysis. **(B)** Dose-response curves for the mouse SIRPA-human CD47-Fc protein interaction determined by SIRPA-CD47 binding assay. Human CD47-Fc protein binding to mouse SIRPA was detected using peroxidase-conjugated goat anti-human Fc antibody. A peroxidase activity was evaluated by the absorbance at 490 nm. $^{**}p < 0.01$. Results shown are representative of four independent experiments. **(C)** Comparison of the amount of phosphorylated SHP-1 in macrophages after exposure to human CD47-Fc protein, as determined by immunoblot analysis.

BALB/c strains on FACS. NOD macrophages bound strongly to human CD47-Fc protein, whereas C57BL/6 macrophages did not, confirming our previous results [16,27]. Interestingly, BALB/c macrophages showed a low level binding capability to human CD47-Fc protein. Figure 1B showed the result of the SIRPA-CD47 binding assay to quantitate the affinity of SIRPA of each strain to human CD47-Fc protein. NOD SIRPA had strong affinity for human CD47 (Kd = 2.501 ± 0.274; Bmax = 0.296 ± 0.005), and BALB/c SIRPA had an intermediate level of affinity (Kd = 306.9 ± 105.2; Bmax = 0.156 ± 0.028), whereas C57BL/6 SIRPA did not bind to human CD47. These results are consistent with those of FACS analysis (Fig. 1A).

It has been shown that the binding of cell-surface CD47 with SIRPA on macrophages activates tyrosine phosphatase SHP-1 to inhibit myosin assembly, preventing engulfment of macrophages [24,25,34,35]. We then tested whether these differences in affinity for SIRPA reflects activation status of SHP-1 phosphorylation after exposure to human CD47-Fc protein (Fig. 1C). The SHP-1 phosphorylation was not detected C57BL/6 macrophages. In contrast, a high level of SHP-1 (68 KDa) phosphorylation was detected in NOD macrophages, and an intermediate level of SHP-1 phosphorylation was seen in BALB/c macrophages. These data suggest that BALB/c macrophages can activate "don't eat me" signaling at an intermediate level because of their modest binding capability to human CD47.

BALB/c-derived macrophages inhibit human LTC-ICs less effectively than C57BL/6-derived macrophages

We have shown that the capability of mouse bone marrow stromal cells to support human LTC-ICs reflects human cell engraftment in vivo in immunodeficient mouse models [16]. It is now clear that macrophages within the stromal cell layer play a critical role in inhibition of LTC-IC maintenance in this experiment. We have found that in long-term culture of human CB cells on MS-5 mouse stromal layer, the addition of C57BL/6 but not NOD macrophages strongly inhibited human LTC-IC maintenance. We therefore analyzed the effect of BALB/c macrophages on human LTC-IC maintenance using this culture system. As shown in Figure 2A, when macrophages from C57BL/6, BALB/c, or NOD were added to the MS-5 stromal layer, this treatment suppressed human LTC-ICs in a dose-dependent manner. The addition of C57BL/6 macrophages was most effective for this suppression that of NOD macrophages was weak ($p < 0.01$), and that of BALB/c macrophages showed an intermediate effect ($p < 0.01$).

To confirm that this difference in inhibition of LTC-ICs is derived from strain-specific *Sirpa* polymorphisms, we cloned the *Sirpa* genes of C57BL/6, NOD, and BALB/c strains, transduced each *Sirpa* lentivirally into C57BL/6 macrophages, and tested their ability to inhibit human LTC-ICs. As shown in Figure 2B, the enforcement of the NOD SIRPA expression in C57BL/6 macrophages strongly

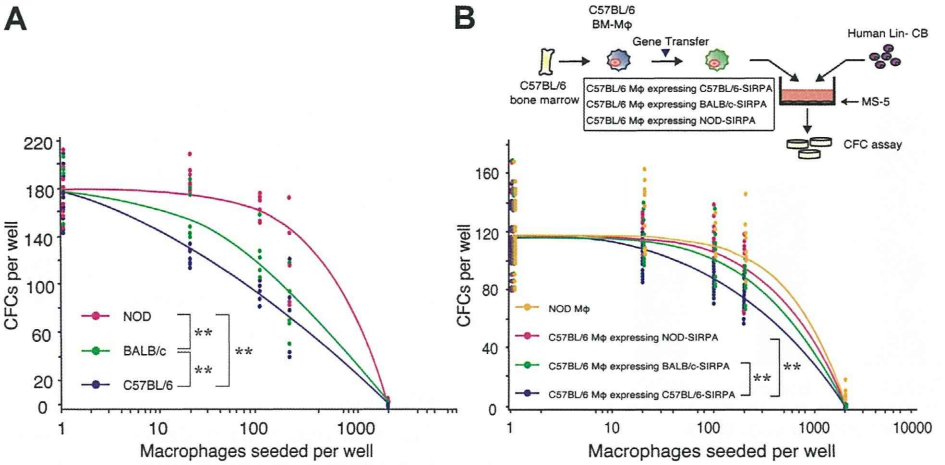

Figure 2. SIRPA modulates mouse macrophage-mediated suppression of human hematopoiesis. **(A)** Inhibition of human LTC-ICs on the MS-5 mouse stromal layer by the addition of macrophages derived from each strain. **(B)** Effects of macrophages with enforced strain-specific SIRPAs on human LTC-IC maintenance. A schematic illustration of the experimental design is shown at the upper panel. $^{**}p < 0.01$. Each experiment was done with five replicates per dose. Results shown are representative of three independent experiments.

restored LTC-ICs, suggesting again that the affinity of SIRPA to human CD47 is a strong determinant of human LTC-IC maintenance in this assay system. Importantly, the enforced expression of BALB/c SIRPA in C57BL/6 macrophages modestly restored the LTC-IC maintenance, reasonably reflecting its intermediate affinity to human CD47.

Engulfment of human HSCs by macrophages is significantly inhibited in the BALB/c strain

Suppression of human LTC-IC maintenance by the addition of mouse macrophages suggests that the target of engulfment should include early hematopoietic progenitor or stem cells. We have shown that in patients suffering from hemophagocytic lymphohistiocytosis (HLH), the $CD34^+CD38^-$ population that is enriched for human HSCs was the primary target of engulfment by activated macrophages to induce pancytopenia [26]. We thus tested whether the intermediate affinity of BALB/c SIRPA to human CD47 can prevent engulfment of human HSCs in vitro. Macrophages of each strain were cultured with human $CD34^+CD38^-$ cells, and the phagocytic index that represents the efficiency of engulfment by macrophages [26,27,32] was evaluated. As shown in Figure 3, C57BL/6 macrophages actively engulfed human HSCs and showed the highest phagocytic index. In contrast, NOD macrophages showed the lowest value, and BALB/c macrophages showed an intermediate value of phagocytic index. Collectively, "don't eat me" signaling induced by a moderate binding of BALB/c SIRPA to human CD47 might prevent engulfment of HSCs by mouse macrophages, which might support LTC-IC maintenance (Fig. 2).

The BALB/c mouse has Sirpa *polymorphism within the IgV domain, which can affect the affinity to human CD47*

The CD47 binding site on SIRPA is located in the distal extracellular IgV loop domain [25,36,37]. We analyzed the IgV domain amino acid sequence of mouse SIRPA to test whether the BALB/c mouse had polymorphisms of the *Sirpa* gene that might affect the binding affinity to human CD47. Critical residues of the *Sirpa* IgV domain for CD47 binding have been determined by multiple mutagenesis analyses in humans and mice [37–40]. X-ray crystallography analyses of human SIRPA-CD47 binding complex revealed that Val27 and Asp100 of human SIRPA IgV are critical for binding [37,38,41], which correspond to Leu29 and Asp104 in mouse SIRPA IgV, respectively (Fig. 4).

The DNA sequence of *Sirpa* IgV domain was determined through PCR amplification of cDNA prepared from the peripheral blood of BALB/c, 129, ICR, and C3H mice. Results are listed in Figure 4, together with data of C57BL6, NOD, NOR *Sirpa*, and human *SIRPA* that were published previously [16]. NOD and BALB/c had common polymorphisms such as Thr4, Val6 and Arg98, but our mutagenesis analysis revealed that these single-nucleotide polymorphisms (SNPs) did not affect its affinity to human CD47 (C. Iwamoto, unpublished data). BALB/c mice had two unique SNPs such as L29V, and substitution of Ile for Val at position 24 (V24I). Because Leu29 in mouse SIRPA corresponds to human Val27, the former substitution could enhance the affinity of mouse SIRPA to human CD47.

We then generated mutant C57BL/6 SIRPA carrying the L29V mutation, enforced to express this mutant in HeLa cells, and evaluated the affinity for human CD47-Fc protein. The affinity of mouse SIRPA to human CD47 was evaluated in the presence of 500 nM of human CD47. As shown in Figure 5A, HeLa cells expressing NOD SIRPA exhibited a strong affinity for human CD47, whereas C57BL/6 SIRPA did not. Cells expressing BALB/c SIRPA showed an intermediate level of affinity. Importantly, cells expressing C57BL/6

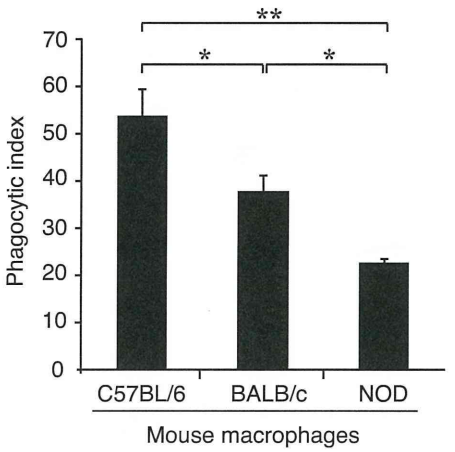

Figure 3. Phagocytosis of human $CD34^{+}CD38^{-}$ hematopoietic stem/progenitor cells by mouse macrophages. The phagocytic index was determined as the number of engulfed cells per 100 macrophages. Bars indicate mean ± SD. $*p < 0.05$; $**p < 0.01$.

SIRPA with the L29V SNP also showed moderate affinity, whose level was comparable to that of cells expressing BALB/c SIRPA. These data strongly suggest that the L29V SNP is an element responsible to enhance the affinity of BALB/c SIRPA to human CD47.

In addition, we evaluated the effect of introduction of L29V SNP on the maintenance of human LTC-IC and the phagocytic activity against human hematopoietic cells, according to the methods used in Figures 2B and 3, respectively. One hundred C57BL/6 macrophages transduced lentivirally with SIRPA of C57BL/6, BALB/c or NOD stains, and with C57BL/6 SIRPA having the L29V SNP, were added to the MS-5 stromal layer. As shown in Figure 5B, by enforcing expression of the C57BL/6 SIRPA with L29V SNP, inhibition of C57BL/6 SIRPA expressing macrophages on human LTC-IC maintenance was significantly released, and became equivalent to that of BALB/c SIRPA-expressing macrophages. The effect of introduction of L29V SNP on the phagocytic activity against human $CD34^{+}CD38^{-}$ stem and progenitor cells is shown in Figure 5C. Consistent with results of the LTC-IC assay (Fig. 5B), macrophages expressing C57BL/6 SIRPA with the L29V SNP showed the phagocytic activity equivalent to that of macrophages expressing BALB/c SIRPA. These findings strongly suggest that BALB/c-specific L29V SNP contributed to the enhanced affinity of BALB/c SIRPA to human CD47, which might cause favorable xenograft efficiencies of human hematopoiesis in the BALB/c strain.

Discussion

Previous studies have shown that mouse strain is an important factor to establish human cell-to-mouse xenotransplantation systems. Like lymphoid-depleted immunodeficient mice of the NOD background, those of the BALB/c strain can support human hematopoietic reconstitution in vivo, although this strain effect is not as strong as the NOD strain does [7,18]. We have shown that the efficient human cell engraftment in the immunodeficient NOD strain is attributable to the NOD-specific *Sirpa* polymorphism [27].

In this study, we show that the polymorphism of the BALB/c *Sirpa* might also be critical to prevent macrophage-mediated suppression of human hematopoiesis. Although a previous report showed that the binding affinity of BALB/c SIRPA for human CD47 was almost absent in the presence of 60 nM of human CD47-Fc protein [42], we found that BALB/c SIRPA showed significant binding affinity at higher concentrations of human CD47-Fc protein (Fig. 1B). The BALB/c-specific polymorphic SIRPA had an affinity for human CD47 at an intermediate level, provoking inhibitory signals such as SHP-1 phosphorylation for macrophages to engulf early hematopoietic stem or progenitor cells, which allowed maintenance of LTC-ICs by MS-5 stromal cells in the presence of BALB/c

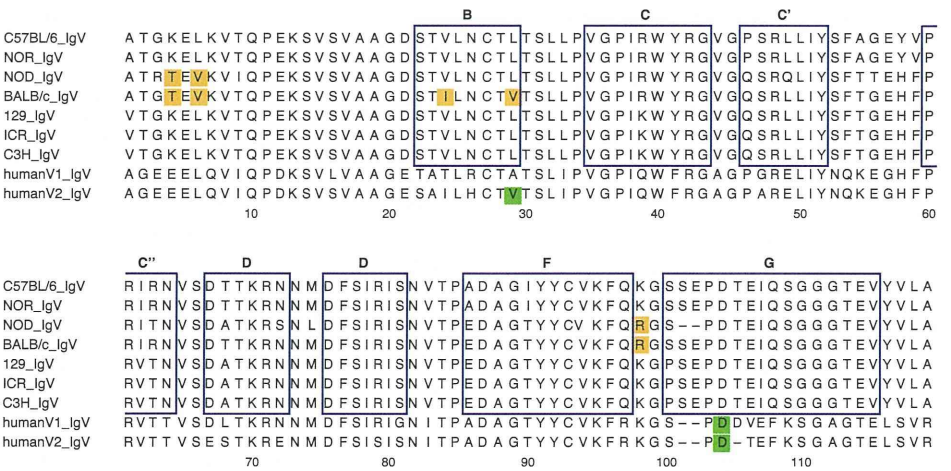

Figure 4. DNA sequencing of the mouse *Sirpa* and human *SIRPA* IgV domain. SNPs specific only to the BALB/c strain, and those to both NOD and BALB/c strains, are boxed in orange. Sequences of the human *SIRPA* IgV domain are aligned to those of the mouse *Sirpa* IgV domain. The residues of human SIRPA critical to bind human CD47 are boxed in green.

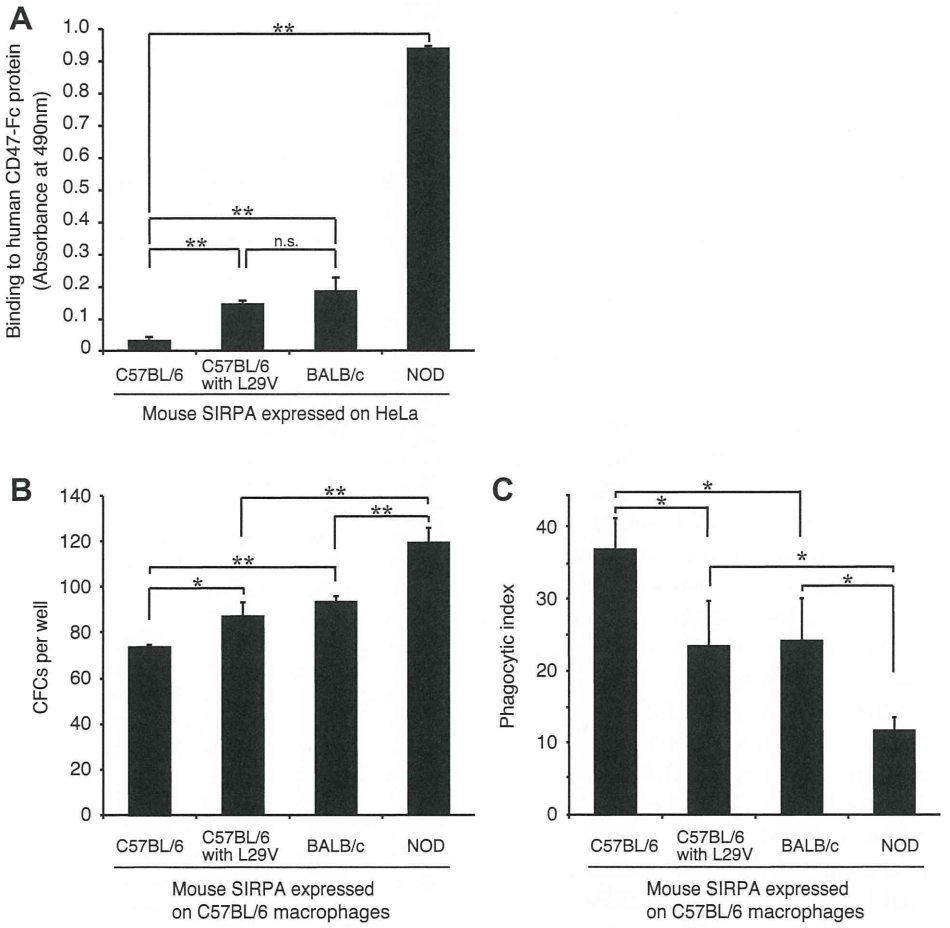

Figure 5. BALB/c-specific SNP L29V confers affinity for human CD47. **(A)** Human CD47-Fc protein binding to HeLa cells infected with C57BL/6, NOD, BALB/c SIRPA, and C57BL6 SIRPA constructs carrying the L29V mutation was evaluated in the presence of 500 nM of human CD47 by a peroxidase activity assay. Binding to human CD47-Fc protein is expressed as a peroxidase activity determined by the absorbance at 490 nm. The results shown are representative of three independent experiments. **(B)** Effects of macrophages with enforced SNP L29V SIRPA on human LTC-IC maintenance. C57BL/6 macrophages expressing strain-specific and SNP L29V SIRPA was added on the MS-5 stromal layer. Each experiment was done with five replicates at a dose of 100 mouse macrophages per well. Results shown are representative of three independent experiments. **(C)** Phagocytosis of human $CD34^+CD38^-$ hematopoietic stem/progenitor cells by mouse macrophages with enforced SNP L29V SIRPA. The phagocytic index was determined as the number of engulfed cells per 100 macrophages. Bars indicate mean ± SD. $*p < 0.05$; $**p < 0.01$.

macrophages. The enforced expression of polymorphic BALB/c SIRPA in C57BL/6 macrophages rendered them unable to inhibit LTC-ICs, and this effect was explainable at least by the L29V SNP of the BALB/c SIRPA. These data strongly suggest that the affinity of strain-specific SIRPA to human CD47 is a decisive factor for efficiency of xenotransplantation.

Interestingly, the degree of the affinity of strain-specific SIRPA appears to correlate with the efficiency of strain-specific transplantation capability. In parallel with an intermediate affinity of BALB/c SIRPA to human CD47, the SHP-1 protein was moderately phosphorylated in BALB/c macrophages, as compared with the level of SHP-1 phosphorylation in NOD macrophages in response to human CD47 (Fig. 1C). It has been reported that human neoplastic cells or leukemic stem cells express higher levels of CD47 than normal cells do, rendering malignant cells to be able to escape from engulfment by macrophages, which endows malignant cells with growth advantages over normal cells [43]. Therefore, in developing efficient xenotransplantation models, further modification of mouse SIRPA to enhance binding to human CD47 should be critical to minimize the inhibitory effect of host macrophages.

It is also important to understand the target cell for engulfment in the xenogeneic transplantation setting. We have reported that disruption of the SIRPA-CD47 binding primarily induces development of human HLH [26]. In HLH, the human $CD34^+CD38^-$ HSC population downregulates CD47 in response to hypercytokinemia, causing HSCs to be engulfed by macrophages. Interestingly, also in the xenogeneic transplantation setting, we showed that the target of engulfment includes the HSC population (Fig. 3). Furthermore, macrophages from the BALB/c mouse engulfed human $CD34^+CD38^-$ cells at an

intermediate level between those seen in the C57BL/6 and in the NOD mouse (Fig. 3), corresponding well to the results of LTC-IC assays (Fig. 2). Thus, the strain-specific inefficiencies for suppression of mouse macrophages should relate directly to the severity of rejection of human HSCs in xenogeneic transplantation models.

The CD47 binding site on SIRPA is located in the IgV loop domain [25,36,37]. The extracellular IgV domain is relatively well conserved (>75%) in both mouse and human SIRPA [37], but the binding to CD47 is species specific. It is probable that the residues at the binding site in the loop domain have a great effect on the shape of the loop by small chemical differences in side chains, resulting in the acquisition of diverse ligand-binding specificities [37,38]. We identified two SNPs unique to BALB/c mice and three SNPs unique to both BALB/c and NOD mice (Fig. 4). Among these five SNPs, the 29th amino acid in mouse SIRPA appeared to be critical because it corresponds to the 27th amino acid in human SIRPA that was critical for human CD47 binding [38–40]. Interestingly, BALB/c and human SIRPA have a Val residue at these sites, whereas all other mouse strains have a Leu residue (Fig. 4). Introduction of C57BL/6 SIRPA carrying the L29V mutation into C57BL/6 macrophages conferred the binding affinity to human CD47 equivalent to that of BALB/c SIRPA, resulting in partial release of human LTC-IC inhibition and phagocytosis against human $CD34^{+}CD38^{-}$ cells (Fig. 5). These results strongly suggest that the L29V mutation contributes to the enhanced binding of BALB/c SIRPA to human CD47 and thus to higher xenograft efficiencies in BALB/c strain, as compared with those in the conventional C57BL/6 strain. Because Val has a slightly shorter hydrophobic side-chain, this exchange could alter conformation of the loop to increase the binding affinity of mouse SIRPA to human CD47.

Conclusion

BALB/c mice have the strain-specific L29V polymorphism in SIRPA, which renders it to be able to recognize human CD47. Our data strongly suggest that one of the critical determinants for strain-specific efficiency of xenogeneic transplantation might be the affinity of the SIRPA-CD47 binding that is decided by strain-specific SIRPA polymorphisms. This information is useful to establish a novel, more efficient immunodeficient mouse models for human cell transplantation.

Acknowledgments

We thank the Japanese Red Cross Kyushu Cord Blood Bank for providing the CB samples. This work was supported in part by a Grant-in-Aid from the Ministry of Education, Culture, Sports, Science and Technology in Japan (to K.A. and K.T.), a Grant-in-Aid from the Ministry of Health, Labour and Welfare in Japan (to K.A.), the Takeda Science Foundation (to K.T.), the Cell Science Research Foundation (to K.T.), the Sumitomo Foundation (to K.T.), the Japan Leukemia Research Fund (to K.T.), and the Uehara Memorial Foundation (to K.A.). We appreciate the technical support from the Research Support Center, Graduate School of Medical Sciences, Kyushu University.

Conflict of interest disclosure

No financial interest/relationships with financial interest relating to the topic of this article have been declared.

References

1. Ishikawa F, Yoshida S, Saito Y, et al. Chemotherapy-resistant human AML stem cells home to and engraft within the bone-marrow endosteal region. Nat Biotechnol. 2007;25:1315–1321.
2. Manz MG, Di Santo JP. Renaissance for mouse models of human hematopoiesis and immunobiology. Nat Immunol. 2009;10:1039–1042.
3. Bhatia M, Wang JC, Kapp U, Bonnet D, Dick JE. Purification of primitive human hematopoietic cells capable of repopulating immune-deficient mice. Proc Natl Acad Sci U S A. 1997;94:5320–5325.
4. Guenechea G, Gan OI, Dorrell C, Dick JE. Distinct classes of human stem cells that differ in proliferative and self-renewal potential. Nat Immunol. 2001;2:75–82.
5. Greiner DL, Hesselton RA, Shultz LD. SCID mouse models of human stem cell engraftment. Stem Cells. 1998;16:166–177.
6. McCune JM, Namikawa R, Kaneshima H, Shultz LD, Lieberman M, Weissman IL. The SCID-hu mouse: murine model for the analysis of human hematolymphoid differentiation and function. Science. 1988; 241:1632–1639.
7. Shultz LD, Schweitzer PA, Christianson SW, et al. Multiple defects in innate and adaptive immunologic function in NOD/LtSz-scid mice. J Immunol. 1995;154:180–191.
8. Shultz LD, Lang PA, Christianson SW, et al. NOD/LtSz-Rag1null mice: an immunodeficient and radioresistant model for engraftment of human hematolymphoid cells, HIV infection, and adoptive transfer of NOD mouse diabetogenic T cells. J Immunol. 2000;164:2496–2507.
9. Shultz LD, Banuelos S, Lyons B, et al. NOD/LtSz-Rag1nullPfpnull mice: a new model system with increased levels of human peripheral leukocyte and hematopoietic stem-cell engraftment. Transplantation. 2003;76:1036–1042.
10. Ito M, Hiramatsu H, Kobayashi K, et al. NOD/SCID/gamma(c)(null) mouse: an excellent recipient mouse model for engraftment of human cells. Blood. 2002;100:3175–3182.
11. Shultz LD, Lyons BL, Burzenski LM, et al. Human lymphoid and myeloid cell development in NOD/LtSz-scid IL2R gamma null mice engrafted with mobilized human hemopoietic stem cells. J Immunol. 2005;174:6477–6489.
12. Ishikawa F, Yasukawa M, Lyons B, et al. Development of functional human blood and immune systems in NOD/SCID/IL2 receptor {gamma} chain(null) mice. Blood. 2005;106:1565–1573.
13. Christianson SW, Greiner DL, Hesselton RA, et al. Enhanced human CD4+ T cell engraftment in beta2-microglobulin-deficient NOD-scid mice. J Immunol. 1997;158:3578–3586.
14. Kollet O, Peled A, Byk T, et al. beta2 microglobulin-deficient (B2m(null)) NOD/SCID mice are excellent recipients for studying human stem cell function. Blood. 2000;95:3102–3105.
15. Ishikawa F, Livingston AG, Wingard JR, Nishikawa S, Ogawa M. An assay for long-term engrafting human hematopoietic cells based on newborn NOD/SCID/beta2-microglobulin(null) mice. Exp Hematol. 2002;30:488–494.
16. Takenaka K, Prasolava TK, Wang JC, et al. Polymorphism in Sirpa modulates engraftment of human hematopoietic stem cells. Nat Immunol. 2007;8:1313–1323.
17. Strowig T, Rongvaux A, Rathinam C, et al. Transgenic expression of human signal regulatory protein alpha in Rag2-/-gamma(c)-/- mice

improves engraftment of human hematopoietic cells in humanized mice. Proc Nat Acad Sci U S A. 2011;108:13218–13223.
18. Brehm MA, Cuthbert A, Yang C, et al. Parameters for establishing humanized mouse models to study human immunity: analysis of human hematopoietic stem cell engraftment in three immunodeficient strains of mice bearing the IL2rgamma(null) mutation. Clin Immunol. 2010; 135:84–98.
19. Ono A, Hattori S, Kariya R, et al. Comparative study of human hematopoietic cell engraftment into BALB/c and C57BL/6 strain of rag-2/jak3 double-deficient mice. J Biomed Biotechnol. 2011;2011: 539748.
20. Hesselton RM, Greiner DL, Mordes JP, Rajan TV, Sullivan JL, Shultz LD. High levels of human peripheral blood mononuclear cell engraftment and enhanced susceptibility to human immunodeficiency virus type 1 infection in NOD/LtSz-scid/scid mice. J Infect Dis. 1995; 172:974–982.
21. Pearson T, Shultz LD, Miller D, et al. Non-obese diabetic-recombination activating gene-1 (NOD-Rag1 null) interleukin (IL)-2 receptor common gamma chain (IL2r gamma null) null mice: a radioresistant model for human lymphohaematopoietic engraftment. Clin Exp Immunol. 2008;154:270–284.
22. Seiffert M, Brossart P, Cant C, et al. Signal-regulatory protein alpha (SIRPalpha) but not SIRPbeta is involved in T-cell activation, binds to CD47 with high affinity, and is expressed on immature CD34(+) CD38(-) hematopoietic cells. Blood. 2001;97:2741–2749.
23. Vernon-Wilson EF, Kee WJ, Willis AC, Barclay AN, Simmons DL, Brown MH. CD47 is a ligand for rat macrophage membrane signal regulatory protein SIRP (OX41) and human SIRPalpha 1. Eur J Immunol. 2000;30:2130–2137.
24. Tsai RK, Discher DE. Inhibition of "self" engulfment through deactivation of myosin-II at the phagocytic synapse between human cells. J Cell Biol. 2008;180:989–1003.
25. Matozaki T, Murata Y, Okazawa H, Ohnishi H. Functions and molecular mechanisms of the CD47-SIRPalpha signalling pathway. Trends Cell Biol. 2009;19:72–80.
26. Kuriyama T, Takenaka K, Kohno K, et al. Engulfment of hematopoietic stem cells caused by down-regulation of CD47 is critical in the pathogenesis of hemophagocytic lymphohistiocytosis. Blood. 2012; 120:4058–4067.
27. Yamauchi T, Takenaka K, Urata S, et al. Polymorphic Sirpa is the genetic determinant for NOD-based mouse lines to achieve efficient human cell engraftment. Blood. 2013;121:1316–1325.
28. Motegi S, Okazawa H, Ohnishi H, et al. Role of the CD47-SHPS-1 system in regulation of cell migration. EMBO J. 2003;22:2634–2644.
29. Enomoto Y, Kitaura J, Shimanuki M, et al. MicroRNA-125b-1 accelerates a C-terminal mutant of C/EBPalpha (C/EBPalpha-C(m))-induced myeloid leukemia. Int J Hematol. 2012;96:334–341.
30. Kagiyama Y, Kitaura J, Togami K, et al. Upregulation of CD200R1 in lineage-negative leukemic cells is characteristic of AML1-ETO-positive leukemia in mice. Int J Hematol. 2012;96:638–648.
31. Okazawa H, Motegi S, Ohyama N, et al. Negative regulation of phagocytosis in macrophages by the CD47-SHPS-1 system. J Immunol. 2005;174:2004–2011.
32. Jaiswal S, Jamieson CH, Pang WW, et al. CD47 is upregulated on circulating hematopoietic stem cells and leukemia cells to avoid phagocytosis. Cell. 2009;138:271–285.
33. Lacks S, Greenberg B. A deoxyribonuclease of Diplococcus pneumoniae specific for methylated DNA. J Biol Chem. 1975;250:4060–4066.
34. Barclay AN, Brown MH. The SIRP family of receptors and immune regulation. Nat Rev Immunol. 2006;6:457–464.
35. Oshima K, Ruhul Amin AR, Suzuki A, Hamaguchi M, Matsuda S. SHPS-1, a multifunctional transmembrane glycoprotein. FEBS Letters. 2002;519:1–7.
36. Hatherley D, Graham SC, Harlos K, Stuart DI, Barclay AN. Structure of signal-regulatory protein alpha: a link to antigen receptor evolution. J Biol Chem. 2009;284:26613–26619.
37. Nakaishi A, Hirose M, Yoshimura M, et al. Structural insight into the specific interaction between murine SHPS-1/SIRP alpha and its ligand CD47. J Mol Biol. 2008;375:650–660.
38. Hatherley D, Graham SC, Turner J, Harlos K, Stuart DI, Barclay AN. Paired receptor specificity explained by structures of signal regulatory proteins alone and complexed with CD47. Mol Cell. 2008;31:266–277.
39. Lee WY, Weber DA, Laur O, et al. Novel structural determinants on SIRP alpha that mediate binding to CD47. J Immunol. 2007;179: 7741–7750.
40. Liu Y, Tong Q, Zhou Y, et al. Functional elements on SIRPalpha IgV domain mediate cell surface binding to CD47. J Mol Biol. 2007;365: 680–693.
41. Hatherley D, Harlos K, Dunlop DC, Stuart DI, Barclay AN. The structure of the macrophage signal regulatory protein alpha (SIRPalpha) inhibitory receptor reveals a binding face reminiscent of that used by T cell receptors. J Biol Chem. 2007;282:14567–14575.
42. Theocharides AP, Jin L, Cheng PY, et al. Disruption of SIRPalpha signaling in macrophages eliminates human acute myeloid leukemia stem cells in xenografts. J Exp Med. 2012;209:1883–1899.
43. Majeti R, Chao MP, Alizadeh AA, et al. CD47 is an adverse prognostic factor and therapeutic antibody target on human acute myeloid leukemia stem cells. Cell. 2009;138:286–299.

Supplementary Table E1. Primer sets to examine the sequences of mouse *Sirpa* CDS and *Sirpa* IgV domains

Name	Primer sequence
C57BL/6 cDNA Sirpa 1F	5′-ATGGAGCCCGCCGGCCCGGCCCCTGGC-3′
C57BL/6 cDNA Sirpa 1R	5′-TCACTTCCTCTGGACCTGGACACTAGC-3′
129 cDNA Exon4 1F	5′-GAGTCACGGGGAAAGAACTG-3′
Exon4R	5′-CGAGTACATAGACCTCTGT-3′
C57BL/6 cDNA Exon3 1F	5′-GCTCTCCGCGTCCTGTTTCTGTACAG-3′
C57BL/6 cDNA Exon5 1R	5′-GGGAGAGAAGCCATGAGACTTGCAGG-3′

THE JOURNAL OF BIOLOGICAL CHEMISTRY VOL. 288, NO. 41, pp. 29333–29344, October 11, 2013

Lack of CD47 Impairs Bone Cell Differentiation and Results in an Osteopenic Phenotype *in Vivo* due to Impaired Signal Regulatory Protein α (SIRPα) Signaling*

Received for publication, June 18, 2013, and in revised form, August 14, 2013 Published, JBC Papers in Press, August 29, 2013, DOI 10.1074/jbc.M113.494591

Cecilia Koskinen[‡], Emelie Persson[‡], Paul Baldock[§], Åsa Stenberg[¶], Ingrid Boström[‡], Takashi Matozaki[‖], Per-Arne Oldenborg[¶], and Pernilla Lundberg[‡1]

From the Departments of [‡]Odontology, Section for Molecular Periodontology, Umeå University, 901 87 Umea, Sweden, the [§]Neurological Diseases Division, Garvan Institute of Medical Research, Darlinghurst, New South Wales 2010, Australia, [¶]Integrative Medical Biology, Section for Histology and Cell Biology, Umeå University, 901 87 Umea, Sweden, and the [‖]Department of Biochemistry and Molecular Biology, Division of Molecular and Cellular Signaling, Kobe University Graduate School of Medicine, Kobe 650-0017, Japan

Background: CD47 and its receptor SIRPα are suggested to regulate bone metabolism.
Results: Lack of CD47 prevents stromal cell SIRPα signaling, which impairs bone marrow stromal cell differentiation, subsequent osteoclast differentiation, and bone homeostasis.
Conclusion: CD47 and SIRPα both mediate normal bone cell and bone tissue formation.
Significance: CD47/SIRPα may be a future molecular target to modulate bone homeostasis.

Here, we investigated whether the cell surface glycoprotein CD47 was required for normal formation of osteoblasts and osteoclasts and to maintain normal bone formation activity *in vitro* and *in vivo*. In parathyroid hormone or 1α,25(OH)$_2$-vitamin D3 (D3)-stimulated bone marrow cultures (BMC) from *CD47*$^{-/-}$ mice, we found a strongly reduced formation of multinuclear tartrate-resistant acid phosphatase (TRAP)$^+$ osteoclasts, associated with reduced expression of osteoclastogenic genes (*nfatc1*, *Oscar*, *Trap/Acp*, *ctr*, *catK*, and *dc-stamp*). The production of M-CSF and RANKL (receptor activator of nuclear factor κβ ligand) was reduced in *CD47*$^{-/-}$ BMC, as compared with *CD47*$^{+/+}$ BMC. The stromal cell phenotype in *CD47*$^{-/-}$ BMC involved a blunted expression of the osteoblast-associated genes osterix, *Alp*/*Akp1*, and α-1-collagen, and reduced mineral deposition, as compared with that in *CD47*$^{+/+}$ BMC. CD47 is a ligand for SIRPα (signal regulatory protein α), which showed strongly reduced tyrosine phosphorylation in *CD47*$^{-/-}$ bone marrow stromal cells. In addition, stromal cells lacking the signaling SIRPα cytoplasmic domain also had a defect in osteogenic differentiation, and both *CD47*$^{-/-}$ and non-signaling SIRPα mutant stromal cells showed a markedly reduced ability to support osteoclastogenesis in wild-type bone marrow macrophages, demonstrating that CD47-induced SIRPα signaling is critical for stromal cell support of osteoclast formation. *In vivo*, femoral bones of 18- or 28-week-old *CD47*$^{-/-}$ mice showed significantly reduced osteoclast and osteoblast numbers and exhibited an osteopenic bone phenotype. In conclusion, lack of CD47 strongly impairs SIRPα-dependent osteoblast differentiation, deteriorate bone formation, and cause reduced formation of osteoclasts.

Resorption of bone is essential for the regeneration of the adult skeleton. After growth, old bone is continuously resorbed by osteoclasts, resulting in bone cavities in which osteoblasts form new bone matrix. This circular process is called remodeling and is a strictly controlled process, which is in balance in a healthy skeletal condition and unbalanced under pathological conditions.

The osteoclast is a bone tissue-specific macrophage polykaryon created by the differentiation of monocyte/macrophage precursor cells in, or in the vicinity of, bone tissue. Osteoclast differentiation is coordinated by bone cells with mesenchymal origin, which include stromal cells, osteoblasts, and matrix-embedded late osteoblasts called osteocytes (1, 2). One of the three known key molecules used by stromal cells/osteoblasts to control osteoclast formation is M-CSF, which binds to c-fms receptors on osteoclast precursor cells and is crucial for the survival and proliferation on these cells. A lack of osteoclasts is observed in osteopetrotic *op*/*op* mutant mice, which lack functional M-CSF (3). The other two cytokines of importance are RANKL (receptor activator of nuclear factor κβ ligand), which binds to RANK (receptor activator of nuclear factor κB) on preosteoclasts, and the decoy receptor osteoprotegerin, which can inhibit osteoclast formation by blocking the interaction between RANKL and RANK (4). Similar to many cytokines and hormones with the capacity to regulate osteoclast formation, the osteotropic hormones parathyroid hormone (PTH)[2] and

* This work was supported by Swedish Research Council 2010-4286 Grant (to P.-A. O.), the Faculty of Medicine of Umeå University, a Young Researcher Award from Umeå University (to P.-A. O.), the Swedish Dental Society, and the County Council of Västerbotten.
[1] To whom correspondence should be addressed: Dept. of Odontology, Sect. for Molecular Periodontology, Umeå University, SE-901 87 Umeå, Sweden. Tel.: 46-90-785-62-94; Fax: 46-90-13-92-89; E-mail: pernilla.lundberg@odont.umu.se.

[2] The abbreviations used are: PTH, parathyroid hormone; BMC, bone marrow culture(s); MEM, minimal essential medium; TRAP, tartrate-resistant acid phosphatase; BMP-2, bone morphogenetic protein 2; PPARγ2, peroxisome proliferator-activated receptor γ2; ALP, alkaline phosphatase; BS, bone surface; ANOVA, one-way analysis of variance; BMM, bone marrow myeloid precursor cell(s).

1α,25(OH)$_2$-vitamin D3 (D3) target osteoblasts and stromal cells causing increased expression and release of RANKL and, therefore, indirectly increase the number of osteoclasts (5). Binding of RANKL to its receptor RANK activates different signaling cascades inducing *nfatc1* (nuclear factor of activated T cells c1), the key transcription factor in osteoclastogenesis. *Nfatc1*, in cooperation with several other transcription factors, induces the transcription of osteoclast-specific genes, including *Trap/Acp5* (tartrate-resistant acid phosphatase), *catK* (cathepsin K), *oscar* (osteoclast-associated receptor), and *ctr* (calcitonin receptor) (5).

Osteoblasts are mononucleated cells derived from pluripotent mesenchymal stem cells, which prior to osteoblast commitment also can differentiate into other mesenchymal cell lineages such as bone marrow stromal cells, fibroblasts, chondrocytes, myoblasts, and adipocytes, depending on the activated signaling transcription pathways. The bone morphogenetic protein 2 (BMP-2) is an example of a potent cytokine, which stimulates osteoblast differentiation and increases bone formation, whereas the peroxisome proliferator-activated receptor γ2 (PPARγ2) is essential in directing the differentiation of adipocyte lineage cells. Activation of the transcription factor Runx2 (Runt-related gene 2) is essential for osteoblast differentiation and bone formation. In addition, the transcription factor osterix, supposed to act downstream of Runx2, and other transcription factors also contribute to the control of osteoblastogenesis. Differentiated osteoblasts express matrix proteins (*e.g.* α-1-collagen) and alkaline phosphatase (ALP), a protein associated with mineralization, which also functions as a biochemical marker for osteoblastic differentiation and bone-forming capacity (6, 7).

CD47, a cell surface glycoprotein of the Ig superfamily and ubiquitously expressed in the body, was originally discovered as an integrin-associated protein important for regulation of at least β1, β3, and β5 integrin members. In addition, CD47 has been suggested to function as a receptor for thrombospondin (8), and as a ligand for signal regulatory protein α (SIRPα) (9). SIRPα is also an Ig superfamily cell surface glycoprotein shown to be highly expressed in myeloid cells, neurons, endothelial cells, and fibroblasts, but not by T cells or B cells. By binding to CD47 on other cells, SIRPα can regulate macrophage-macrophage adhesion, fusion, and formation of giant cells (10, 11).

We have previously shown that osteoclast formation is reduced both *in vivo* and *in vitro* in the absence of CD47 (12). These findings have been confirmed *in vitro* both by Uluçkan *et al.* (13) and Maile *et al.* (14). However, Maile *et al.* did not find any reduction in number of osteoclasts *in vivo* (14). To determine the role of CD47 in bone homeostasis, both *in vitro* and *in vivo*, we here investigated whether CD47 is involved in osteoclast and stromal cell/osteoblast differentiation in murine bone marrow cultures. In addition, we studied osteoblast numbers and bone homeostasis in *CD47*$^{-/-}$ mice.

EXPERIMENTAL PROCEDURES

CD47$^{-/-}$ *Mice and SIRPα Mutant Mice*—Generation of *CD47*$^{-/-}$ has been described previously (15). Male *CD47*$^{-/-}$ Balb/c mice, backcrossed to Balb/c (The Jackson Laboratory, Bar Harbor, ME) for 16 or more generations, and their wild-type homozygous littermates were from our own breeding colony. C57BL/6 SIRPα mutant mice, lacking most of the SIRPα cytoplasmic domain were described previously (16, 17). Male SIRPα mutant mice or their wild-type littermates, backcrossed for >10 generations, were from our own breeding colony. Animals were kept in accordance with local guidelines and maintained in a specific pathogen-free barrier facility. The Local Animal Ethics Committee approved all animal procedures.

Bone Marrow Cell Culture (BMC)—Bone marrow cells were isolated from femurs and tibiae of Balb/c mice, 5–9 weeks of age (*CD47*$^{+/+}$ and *CD47*$^{-/-}$) and seeded on 48- or 12-well plates (Nunc, Roskilde, Denmark) in α-MEM with 10% FCS (Invitrogen), L-glutamine, and antibiotics (Sigma Aldrich), with cell concentration of 10^6 cells/cm^2. The number of mice used for each experiment differed between 1–4 depending on the size of the experiment. If more than one mouse was used, the bone marrow cells were pooled. After 24 h (day 0) of incubation (37 °C, 5% CO_2), the medium was replaced and either PTH 10^{-8} M (Bachem, Bubendorf, Switzerland), D3 10^{-8} M (Roche Diagnostics, Mannheim, Germany), or BMP-2 125 ng/ml (R&D Systems, Abdingdon, UK) were added to the cultures. At day 3, medium and test substances were changed. On days 6–7, the cultures were harvested, and the cells were either lysated for further RNA isolation or fixed with acetone in citrate buffer and subsequently stained for TRAP as described below.

Osteoclast Formation and Resorption on Bone Slices—Bone marrow cells were isolated as described above. Thereafter, the cells were seeded on bone slices in 96-well tissue culturing plates (Nunc, Roskilde, Denmark) in α-MEM with 10% FCS (Invitrogen), L-glutamine and antibiotics (Sigma Aldrich), with cell concentration of 10^6 cells/cm^2. The cells were incubated for 24 h (37 °C, 5% CO_2), and thereafter, the medium was changed and D3 10^{-8} M (Roche Diagnostics) was added. Medium was changed every third day, and after 10 days of culture, the experiments were harvested and stained for TRAP positivity, osteoclasts were counted in a light microscope, and resorption pits were visualized by an external light source. Moreover, the release of collagen type I fragments into the culture medium during resorption was analyzed by CrossLaps according to the manufacturer's instructions.

Osteoblast Differentiation—Bone marrow cells were isolated and plated as in above described BMC and plated in 24-well tissue culturing plates (Nunc, Roskilde, Denmark). The cells were cultured in α-MEM with 10% FCS (Invitrogen), L-glutamine, and antibiotics (Sigma Aldrich). The medium was changed every third day. At day 6, the culture medium was replaced with osteoblastic differentiation medium (α-MEM with 10% FCS, L-glutamine, antibiotics, 10 mM β-glycerol phosphate, and 50 μg/ml ascorbic acid). At days 7, 14, and 21, the cells were fixed with acetone in citrate buffer and stained for ALP or von Kossa as described below.

Bone Marrow Stromal Cell Culture—Bone marrow cells were isolated and treated as in BMC except that they were plated in 60 cm^2 culture dishes (Nunc). The cells were cultured in α-MEM with 10% FCS (Invitrogen), L-glutamine, antibiotics (Sigma Aldrich). The medium was changed after 3 days. After 7 days, the adhering cells were detached, counted, and plated at a concentration of 2×10^4 cells/cm^2 in 24-well and 12-well tissue

culturing plates (Nunc). The cells were either lysed for further RNA isolation or stained for ALP or von Kossa at the stated culture time.

Co-culture—Cells used for co-culture experiments were harvested from mice, 5–9 weeks of age, either Balb/c ($CD47^{+/+}$ and $CD47^{-/-}$) or C57BL/6 wild-type or SIRPα mutants. Bone marrow cells were isolated and treated as in BMC except that they were plated in 60 cm^2 culture dishes (Nunc). The cells were cultured in α-MEM with 10% FCS (Invitrogen), L-glutamine, and antibiotics (Sigma Aldrich). Medium was changed every third day, and after 14 days, the adherent cells were trypsinated, counted, and seeded at 10^5 cells/cm^2, in 96-well tissue culturing plates (Nunc) and thereafter incubated for 24 h (37 °C, 5% CO_2). Meanwhile non-adherent bone marrow myeloid precursor cells were isolated by flushing out bone marrow from femurs and tibiae. Following lysis of erythrocytes, the remaining cells were plated in 60 cm^2 tissue culture-treated culture dishes (Nunc) and kept at 37 °C for 2 h. Thereafter, the non-adherent cells were collected, counted, and seeded onto the stromal cells at 6×10^4 cells/cm^2. The co-cultures were stimulated with D3 10^{-8} M (Roche Diagnostics, Mannheim, Germany). After 5–7 days, the cultures were harvested, fixed, and stained for TRAP as described below.

TRAP staining was performed by use of the leukocyte acid phosphatase kit (Sigma-Aldrich) according to the manufacturer's instructions. $TRAP^+$ cells with three or more nuclei were considered osteoclasts, and the number of multinucleated osteoclasts was counted in a light microscope.

ALP and von Kossa Staining—Osteoblast differentiation was visualized with ALP staining by using Naphtol AS-MX phosphate, disodium salt, and Fast Blue BB (Sigma Aldrich) according to histochemical standard procedure. Mineralization of extracellular matrix was visualized by von Kossa staining with 2% silver nitrate (Fisher Scientific UK) under UV light for 30 min. The result of ALP and von Kossa staining was photographed.

RNA Isolation and First-stranded cDNA Synthesis—Total RNA from adherent bone marrow cell cultures was isolated by using the RNAqueous®-4PCR kit (Ambion, Austin, TX) according to the manufacturer's instructions. By using the high capacity cDNA reverse transcription kit (Foster City, CA), mRNA was reverse-transcribed to cDNA.

Quantitative Real-time PCR—To detect and analyze gene expression, Taq-man (API PRISM 7900HT Sequence Detection System) was used. The expression of *Trap/Acp5*, *ctr*, *catK*, *nfatc1*, *oscar*, *dc-stamp*, *c-fms*, *rank*, *rankl*, *m-csf*, *SIRPα*, *runx-2*, osterix, α-1-collagen, *Alp/Akp1*, *PPARγ* and osteoprotegerin were analyzed in BMC. To control variability in amplification due to differences in starting mRNA-concentrations, β-actin was used as housekeeping gene.

ELISA—The amount of synthesized protein of RANKL and M-CSF in culture medium was assessed by measuring the levels of the proteins in BMC using commercially available ELISA kits. RANKL was measured according to manufacturer's instructions (R&D Systems) and M-CSF according to the manufacturer's instructions (AB Frontier, Seoul, Korea).

TRAP Activity Assay—BMC were washed three times in PBS and lysed in Triton X-100 (0.2% in H_2O). By using *p*-nitrophenol phosphate (1.7 mg/ml) as substrate at pH 4.9 in the presence of tartrate (0.17 M), the TRAP activity was determined. The activity of the enzyme was assessed as the A_{405}. The enzyme assay was performed under conditions where the reaction was proportional to amount of enzyme and reaction time.

ALP Activity Assay—Alkaline phosphatase was measured in BMC stimulated with BMP-2 by using a commercially available kit (Sigma Aldrich).

Flow Cytometric Analysis—Bone marrow stromal cells were washed and resuspended in cold PBS. Fifty μl of the cells (1×10^5 cells) were seeded in a 96-well V-bottomed plate and centrifuged at 1500 rpm for 3 min at 4 °C. Thereafter, the cells were resuspended in 30 μl staining buffer (PBS + 2% FCS) containing saturating concentrations of Alexa Fluor 488-conjugated anti-SIRPα mAb P84, or Alexa Fluor 488-conjugated rat IgG isotype control mAb, for 30 min on ice. Cells were then washed once with 200 μl of cold PBS, resuspended in cold PBS/2% FCS/0.05% NaN_3, and analyzed by flow cytometry (FACS Calibur, Becton Dickinson) and CellQuest software (Beckton Dickinson).

Immunoprecipitation and Western Blot—Bone marrow stromal cells, cultured for 14 days, were lysed with ice-cold lysis containing 20 mM Hepes (pH 7.4), 150 mM NaCl, 1 mM EGTA, 1% Nonidet P-40 (Pierce), 1% of proteinase inhibitor mixture (Sigma), 0.5 μM pervanadate, and 1 mM phenylmethylsulfonyl fluoride. Immunoprecipitation with the anti-SIRPα mAb P84 was done essentially as described previously. In brief, cell lysates were incubated with mAb P84-coated protein G-Sepharose overnight at 4 °C. Washed immunoprecipitates were boiled for 5 min in reduced SDS-PAGE sample buffer with β-mercaptoethanol and separated on 10% SDS-PAGE, followed by transfer to nitrocellulose under standard conditions. Nonspecific binding was blocked by 3% nonfat dry milk in TBST (50 mM Tris, 150 mM NaCl, 0.1% Tween 20 (pH 7.6)) followed by immunoblotting with anti-SIRPα mAb P84 or anti-phosphotyrosine mAb 4G10 (Millipore). Primary antibodies were detected with peroxidase-conjugated goat anti-rat or anti-mouse mouse IgG, and detection of signals was by chemiluminescence (ECL, Amersham Biosciences).

Phenotypic Studies—Histomorphometry and peripheral quantitative computed tomography were used to analyze the bone phenotype of male BalbC $CD47^{-/-}$ mice at the age of 18 and 28 weeks and compared with normal mice at the same age.

Histomorphometry—$CD47^{+/+}$ or $CD47^{-/-}$ mice were injected with the fluorescent compound calcein (15 mg/kg; Sigma) 10 days and 3 days prior to collection, respectively. At 18 and 28 weeks of age $CD47^{+/+}$ and $CD47^{-/-}$ were euthanized by cervical dislocation. Both femurs were excised and bisected transversely at the midpoint of the shaft. The distal halves of the right femora were fixed and embedded, undecalcified in methyl-methacrylate resin (Medim-Medizinische Diagnostik, Giessen, Germany), and 5-μm sagittal sections were prepared for analysis using Q Win software (Leica Microsystems Pty., Ltd., Sydney, Australia). Sagittal sections were stained for mineralized tissue, and trabecular bone volume, trabecular thickness, and trabecular number were calculated in a sample region extending 4.5 mm proximal to the distal growth plate and encompassing all trabecular bone within the cortical boundaries. Osteoblast